away from that status at the time of this writing. Thus, it is crucial to identify whether the upturn in Japan is qualitatively similar to those observed in the US and Europe.

However, whereas the upturns in the US and Europe are generally considered to have occurred because the period TFR returned to the long-term cohort TFR as tempo effects die out due to completion of postponement transition (Goldstein et al. 2009), it is suggested that the upturn being observed in Japan is of a different nature and is caused by other, peculiar causes.

From a long-term perspective, if the rise in fertility currently being observed is purely caused by type-H period effects, the period fertility rate should decline again within the next several years and will ultimately not significantly change the long-term outlook for the fertility rate. In fact, according to observation of the monthly development, fertility rates have already been turning around to a downward trend again for at least eleven months since December 2008.

On the other hand, this downturn itself might have been caused by transient disturbances related to the financial crisis starting roughly in September 2008 (Goldstein et al. 2009) and may actually be indicative of a complicated situation where different period effects overlap in some way.

Meanwhile, if the circumstances that brought about the recent upturn also serve to keep the fertility rates at higher levels than in the past for an extended period of time, overcoming this transient period of decline, the end result will be a positive influence on the cohort fertility, where the long-term outlook will involve a higher fertility than in the past. In this case, current period effects are modified from type-H to type-H'.

Therefore, it is important to attempt to understand the causes of the upturn. According to the analysis of observed age-specific fertility rates, the main players in the recent reversal are the so-called second baby boomers, i.e., the generation born in the period from 1971 to 1974. The second baby boomers were expected to give birth to the third baby boomers in the latter half of the 1990s and onward. However, this event was never realized due to significant postponement of family formation and/or childbearing.

On the contrary, their fertility rates kept on falling in 2000 and onward as well and reached the lowest low level in 2003. However, eventually it likely became clear to members of this group that if they wished to have a certain number of children in their lives, they were approaching the age limit to realize this desire. This childbearing urge should have reached super-saturation in 2003 and onward. Assuming these conditions hold, it appears that pregnancy and childbirth were further suppressed from 2004 to the first half of 2005 for some reason. One can thus imagine that excessive energy recoil had been accumulated.

Continuing this line of thought, it is possible that the changes in the social economic mood, which among other things involved a generally improved employment environment, triggered the sudden release of this pent-up desire among the second baby boomer generations.. In other words, although the trigger itself was a very ordinary change, there is a distinct possibility that it led to abrupt, significant changes in the trend due to the interaction with the circumstances of the players.

If that is the case, the decline of fertility from around 2003, particularly the drop in 2005, was caused by type-H period effects in the negative direction and the rise afterward occurred as a rebound to the decline, caused by type-H period effects in the positive direction. Note that the recent rise is actually accelerating and is exceeding the level of the rebound in 2004 to 2005, suggesting the possibility that additional factors are involved.

For example, the large-scale second baby boomer generation's growing desire to get married and/or have children itself forms a market demographic and is likely to gather momentum through mass media and similar channels. Magazines targeting women aged 30 years and up began to feature many positive articles featuring marriage, pregnancy, childbirth, and childrearing, and fashionable new words related to

such subjects are becoming commonplace[1]. Furthermore, the national government and local governments are advertising their measures to promote childbearing as well. Spearheaded by the mass media, such measures seem to form a positive feedback relationship with the increasing fertility. Namely the initial rise from the rebound caused an increase in media coverage about marriage and family, which in turn promoted further marriages and caused additional births to occur.

What will happen to this reversal trend of fertility in the future? First, if the rise in most cohorts ends up as a simple type-H period effect from rebound and temporary boom, the fertility rates will regress on the line of the previous prospect. In this scenario the recent boom comes to an end soon and it becomes difficult to maintain the current level when the fertility starts to stagnate and the feedback cycle with popular culture is cut. Signs hereof may be already beginning to show in the monthly development.

On the contrary, if the boom continues for long enough to make the increases type-H' and so raise the levels of completed fertility, and if those age patterns are continually succeeded by the following cohorts, then it means that the shrinking trend of cohort fertility reverses and the long term prospects of fertility should be revised to be as high as improved level of cohort completed fertility. In this case, the feedback relationship would be maintained. It is possible the group of single people and families of under-parity has ballooned to a huge size by now, because it contains the second baby boomers.

There are several other factors affecting the future course of fertility, among which the new child allowance is particularly notable. The new government has promised the adoption of this policy, and it amounts to 26,000 yen (about 290 US dollar) a month per every child through junior high. The current plan is to enact half the amount of allowance in April 2010, and the full amount in April 2011. Though it may have a certain impact on fertility, it seems necessary that it be perpetual and publicly viewed as reliable to alter the long term trends beyond just period fertility in the short term.

7. Conclus ion

In this paper, we pursued three objectives: (1) to show the usefulness of population projection models in analyzing demographic processes in the past and present as well as in the future, (2) to measure and understand the period effects in terms of modifiers of the cohort fertility schedule, and (3) to identify factors and mechanisms of the recent peculiar fertility development in Japan, using the proposed framework.

Fertility projection is utilized to analyze the period effects that are latent within the past and current fertility trends. It seems that the framework is useful to separate out the type-H and H' period effects from the type-T period effects (the tempo effects) and cohort effects so that causes of changes in fertility trend may be identified.

The fertility rates in Japan have dropped continuously below the replacement level from the mid 1970s until 2005, and Japan experienced the so-called lowest low fertility for a three-year period from 2003 to 2005. However, in the recent three years from 2006 to 2008, an upturn trend has been observed in the fertility rates, and the TFR rose to 1.37 in 2008.

Using the period effect analysis composed with the fertility projection system, it is estimated that the recent upturn can mainly be explained by the period effect, which does not change cohort completed fertility, and particularly the effects that cause temporal shifts and are redeemed in other periods (termed the period effect of type-H). For some cohorts in higher ages, however, it is likely the completed fertilities become slightly larger than previously estimated as a result of the type-H' effect. These are different in causes from the upturns seen in the US and Europe, where the period fertility rates have been reversed mostly by "the tempo transition" (Goldstein et al 2009) which is the completing phase of the

[1] "Kon-katsu" (activities to look for marriage partners) - there is affirmative nuance for the activities. "Ara-for"(Around Forty) - a somewhat positive title for single women around age 40, who are typically active in work and romance. "Sosyoku-danshi" (herbivorous boy) – a label for young men who are passive to romance and marriage, suggesting that women should be active to make those come into existence.

"postponement transition"(Kohler et al 2002). This corresponds to the period effect of type-T in our terminology.

The upturn in Japan seems to be caused by a rebound of the short term too-low fertility in the lowest low period, or in 2003-2005, followed by a boom induced mainly by the media targeting the single's and family of under parity's market whose size is unprecedented in these years, partly because it includes the second baby boomers.

It is possible that the long term prospects of fertility formed in the latest population projection, which are based on the data corrected by the year 2005, might be underestimated in light of the present situation. It depends on whether the rise in fertility schedules of cohorts in their mid-thirties and beyond in this period is continually succeeded by the following cohorts ending up with rises in their cohort completed fertilities.

References

Billari, Francesco C. (2008). Lowest-low fertility in Europe: Exploring the causes and finding some surprises. *Japanese Journal of Population* (Tokyo) vol.6, No.1, pp. 2-18.

Bongaarts, John and Griffith Feeney (1998). On the quantum and tempo of fertility. *Population and Development Review* (New York) vol.24, No.2, pp.271-291.

Goldstein Joshua R. Tomáš Sobotka, and Aiva Jasilioniene (2009). The end of 'lowest-low' fertility? Paper presented at the XXVI IUSSP International Population Conference, Marrakech.

Kaneko, Ryuichi (2003). Elaboration of the Coale-McNeil nuptiality model as the generalized log gamma distribution: A new identity and empirical enhancements *Demographic Research* (Rostock) Vol. 9, No. 10, pp.223-262. http://www.demographicresearch.org/Volumes/Vol9/10/9-10.pdf

Kaneko, Ryuichi, Akira Ishikawa, Futoshi Ishii,Tsukasa Sasai, Miho Iwasawa, Fusami Mita, and Rie Moriizumi (2008). Population projections for Japan: 2006-2055: outline of results, methods, and assumptions. *The Japanese Journal of Population* (Tokyo), Vol.6, No.1, pp.76-114. http://www.ipss.go.jp/webj-ad/WebJournal.files/population/2008_4/05population.pdf

Kohler, Hans-Peter, Francesco C. Billari, and José A. Ortega (2002). The emergence of lowest-low fertility in Europe during the 1990s. *Population and Development Review* (New York) vol.28, No.4, pp.641-680.

National Institute of Population and Social Security Research (NIPSSR), 2007. *Nihon no Syorai Suikei Jinko* (*Population Projection for Japan: 2006-2055*), Tokyo: Kosei Tokei Kyokai.

Sobotka, Tomáš (2004). Is lowest-low fertility explained by the postponement of childbearing? *Population and Development Review* (New York) vol.30, No.2, pp.195-220.

van Imhoff, Evert (2001). On the Impossibility of Inferring Cohort Fertility Measures from Period Fertility Measures, *Demographic Researc* (Rostock) Vol. 5, No. 2, pp. 24-64. http://www.demographic-research.org/Volumes/Vol5/2/5-2.pdf

APPLICATION OF AGE-TRANSFORMATION APPROACHES TO MORTALITY PROJECTION FOR JAPAN

Futoshi ISHII[1]

Introduction

For projecting future mortality in "Population P rojection for Japan: 2006-2055" (NIPSSR 2007), a n ew "age-shifting model", which incorpor ates age-shifting as well as age- scaling of m ortality, has been developed and used (I shii 20 08). These kin ds of ope rations c ould be i ncorporated int o a m ore ge neral framework, i.e. an age-transformation approach.

This paper serves to examine and propose a novel method for the mortality projection of Japan that is an application of the age-transformation approach.

1. Two Representations of the Log Mortality Surface

In this section, we discuss two representations of the log mortality surface and define certain functions to describe the log mortality and its inverse functions.

Let $X = [0, +\infty)$ be the space of a ge and $T = (-\infty, +\infty)$ be the space of tim e. In the following discussion for modeling mortality, we will use $\mu_{x,t}$ the hazard function for exact age $x \in X$ at tim e $t \in T$. In this paper, we e xpress the log hazard function of m ortality as $y = \lambda_{x,t} = \log \mu_{x,t}$, w here $y \in Y = (-\infty, +\infty)$ is the value of the function. Then, th e s et $S = \{(x,t,y) | y = \lambda_{x,t}\}$ determ ines a surface in $\Re^3$, called the *log mortality surface*. This is a conventional representation of the log mortality surface. In thi s repre sentation, $y = \lambda_{x,t}$ woul d be c onsidered as the heig ht fr om the $X - T$ plane in $\Re^3$.

Here, we consider another representation of the log mortality surface under a set of assumptions.

We assum e that $\lambda_{x,t}$ is a s mooth continuous function with respect to x and t defined o n $X_0 \times T_0 = [0, \omega] \times [t_0, t_1] \subset X \times T$, where $\omega < +\infty$ is the finite maximum age for mortality models.

For the purpose of m odeling *adult* mortality, we can furt her assum e that $\lambda_{x,t}$ exhibits a strictly monotonic inc rease with respect to x for e ach t and $x > x_0(t)$. He re, $x_0(t)$ represents the lowe r

[1] National Institute of Population and Social Security Research

bound of x above which $\lambda_{x,t}$ exhibits a strictly monotonic increase for each t. Then, for each t, the function $\lambda_t(x)$ defined by

$$\lambda_t : \tilde{X}_t \to Y, \quad \lambda_t(x) \underset{\text{def}}{=} \lambda_{x,t}$$

is the injective (one to one) function of x, where $\tilde{X}_t = [x_0(t), \omega]$. Let $\tilde{Y}_t = \lambda_t(\tilde{X}_t)$, then $\lambda_t(x) : \tilde{X}_t \to \tilde{Y}_t$ has an inverse function $v_t(y) : \tilde{Y}_t \to \tilde{X}_t$ defined on $\tilde{Y}_t$ for each t.

Let us define Y_0 as follows:

$$Y_0 \underset{\text{def}}{=} [y_0, y_1] \text{ where } y_0 = \sup_{t \in T_0} \min \tilde{Y}_t, \qquad y_1 = \inf_{t \in T_0} \max \tilde{Y}_t$$

Then, we can define $v_{y,t} : Y_0 \times T_0 \to X_0$ by $v_{y,t} \underset{\text{def}}{=} v_t(y)$

$v_{y,t}$ gives the *age* x at which the value of the log hazard function is equivalent to a value y at time t. Moreover, we define the following two differential functions by time t: (1) $\rho_{y,t}$: the mortality improvement rate and (2) $\tau_{y,t}$: the force of age increase.

$$\rho_{x,t} \underset{\text{def}}{=} -\frac{\partial \lambda_{x,t}}{\partial t} = -\frac{\partial \log \mu_{x,t}}{\partial t}$$

$$\tau_{y,t} \underset{\text{def}}{=} \frac{\partial v_{y,t}}{\partial t}$$

2. Age-transformation

Next, we introduce an age-transformation in mortality analysis. In this paper, we define the age-transformation as follows.

Def 1. Let $x, z \in [0, \infty)$ be coordinates for age. If we have a transformation $f_t : z \to x$, which is continuous and monotonically increasing, we call f_t as an age-transformation from x to z at time t.

Let us consider graphical representations of the age-transformation. We use the following two representations, the graph of $x = f_t(z)$ and an "iso transformed-age map".

Here, we look at these graphs with an example of shifting age-transformation, which is defined by the following equation.

$$x = f_t(z) \underset{\text{def}}{=} \max(5t + z, 0) \quad (t = -2, -1, 0, 1, 2)$$

The relationship among x, z and t is expressed in three-dimensional space as shown in Figure 1.

One way to project this relationship onto two-dimensional space is by plotting the graph of $x = f_t(z)$ for each t on the X-Z plane. Figure 2 illustrates this graph. From this, we are able to read which age in the original coordinate (x) corresponds to the transformed one (z).

Another way to project onto two-dimensional space is to consider which ages in the original coordinate are identified by this transformation. We can express this by showing a plot $f_t(y)$ for $y = 0, 1, \cdots, 110$. We call it "iso transformed-age map". Figure 3 is the iso transformed-age map for this shifting age-transformation. The red lines shows the age 0, 10, ..., 110.

Figure 1: Relationship between x, z *and t* (shifting)

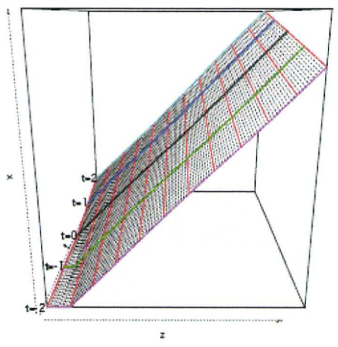

Figure 2. Age-transformation Function (shifting)

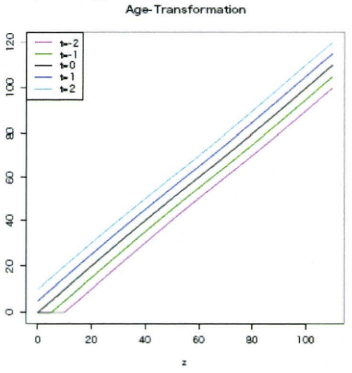

Figure 3. Iso Transformed-age Map (shifting)

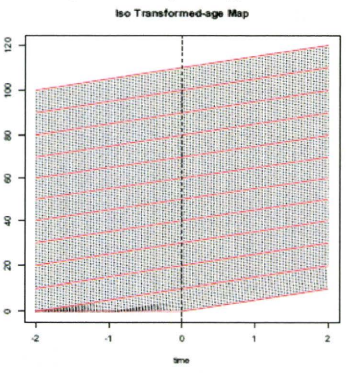

3. Lee-Carter model and Age-transformation Approach

In Section 2, we introduced an age-transformation approach for mortality analysis. In this section, we review our preceding work for Japanese mortality projection that combined the Lee-Carter model with age-transformation (Ishii 2008).

The Lee-Carter model (abbreviated as LC) is expressed by the following formula (Lee and Carter 1992).

$$\lambda_{x,t} = \log \mu_{x,t} = a_x + k_t b_x$$

where a_x is a standard age pattern of mortality.

Taking a partial derivative by time t, we obtain the following relationship.

$$\rho_{x,t} \underset{\text{def}}{=} -\frac{dk_t}{dt} b_x = -k_t' b_x$$

This equation shows that the age distribution of $\rho_{x,t}$ is constant in the LC model. If we further assume that k_t is linear over time, $\rho_{x,t}$ is constant over time. Therefore, the LC model works well when the age-specific rate of mortality improvement is considered to be constant over time, that is, the mortality improvement is considered as *decline*.

Then, when does the LC model fail to express mortality improvement? To observe this point, we examine the following stylized examples.

Here, we consider two piecewise linear log mortality functions. At $t = 0$, both functions are identical: $\lambda_{x,t} = -2$ for age 0, -8 for age 25, -6 for age 50, -3 for age 75 and -1 for age 100. In Example 1, age-

specific rates of improvement are constant over time. The annual rate of decline is 0.12 for age 0, 0.06 for age 25, 0.06 for age 50, 0.07 for age 75 and 0.04 for age 100.

In Example 2, age-specific rates of improvement for ages under 25 are constant and the same as in Example 1. However, for ages above 50, the mortality curve shifts to the right 3/5 years annually.

Figure 4 shows $\lambda_{x,t}$ (top figure) and $\rho_{x,t}$ (bottom figure) for Example 1. From the bottom figure, we can observe that the rates of mortality improvement are constant over time.

Figure 5 shows the same figures for Example 2. From the bottom figure, we can observe that the peak of the rates of mortality improvement is shifting to the right over time. Such mortality improvement could not be expressed by the LC model. The black line shows the rate of mortality improvement, which is equal to the b_x function under the LC model. We can observe that this line exhibits an average rates of mortality improvement for the entire period, even though no actual $\rho_{x,t}$ shows such rates of mortality improvement.

Figure 4. $\lambda_{x,t}$ and $\rho_{x,t}$ Example 1

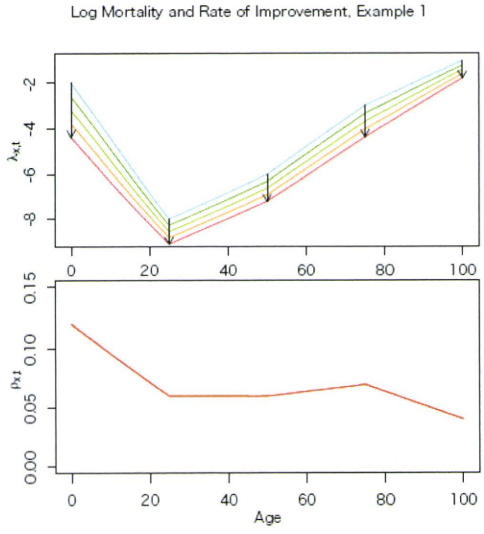

Figure 5. $\lambda_{x,t}$ and $\rho_{x,t}$ Example 2

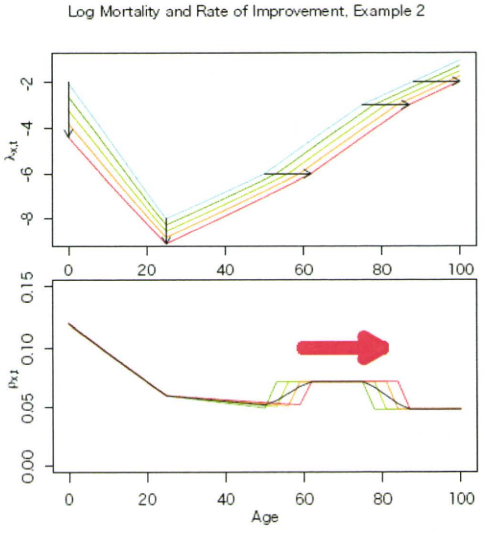

Following these observations, we could say that use of the LC model may not be considered appropriate if the mortality improvement is considered as *shifting*. We proposed age-transformation approaches for projecting Japanese mortality rates since we observed the recent mortality improvement in Japan could be considered as *shifting*, though this point is reconsidered later.

The age-transformation approach works as follows. Let us denote the LC modeling and projecting procedure as *L*; then the modeled and projected mortality $\hat{\mu}_{x,t}$ by the LC procedure would be obtained as $L(\mu_{x,t})$. We proposed performing the Lee-Carter procedure after some age-transformation, and modelling and projecting the rates by inverse age-transformation, i.e., $A^{-1}L\,A(\mu_{x,t})$.

[Lee-Carter model]

$$\mu_{x,t} \;\downarrow\; \mathcal{L} \;\downarrow\; \hat{\mu}_{x,t}$$

[Lee-Carter model with Age-transformation]

$$\begin{array}{ccc} \mu_{x,t} & \xrightarrow{\;A\;} & \beta_{z,t} \\ & & \downarrow \mathcal{L} \\ \hat{\mu}_{x,t} & \xleftarrow{\;A^{-1}\;} & \hat{\beta}_{z,t} \end{array}$$

Here, we illustrate how the age-tran sformation approach will work in Example 2. Let us consi der the following age-tran sformation: shifting m ortality curves to the left 3/5t y ears for the group aged 50 and over as in the top figure in Figure 6. Then the transformed mortality rates are in the bottom figure.

Figure 7 shows the a ge-transformed $\lambda_{x,t}$ and the rates of m ortality improvement $\rho_{x,t}$. We can see that the $\rho_{x,t}$ function for the age-transformed m ortality is constant over ti me, and thus the LC model provides a perfect fit for the age- transformed mortality rates. Therefore, we can model Example 2 using the LC model with age-transformation. This is a core structure of this approach.

Figure 6. Age-transformation for Example 2

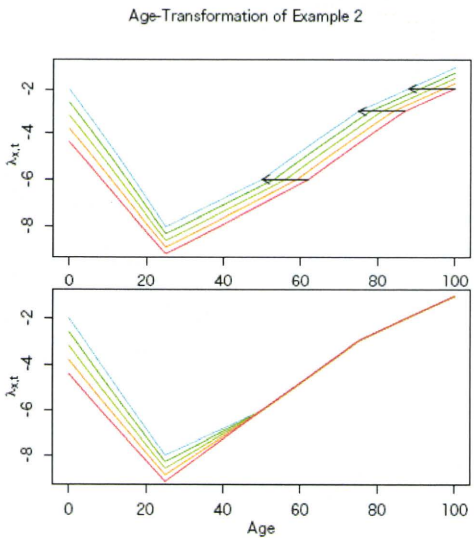

Figure 7. $\lambda_{x,t}$ and $\rho_{x,t}$ Example 2 (with Age-transformation)

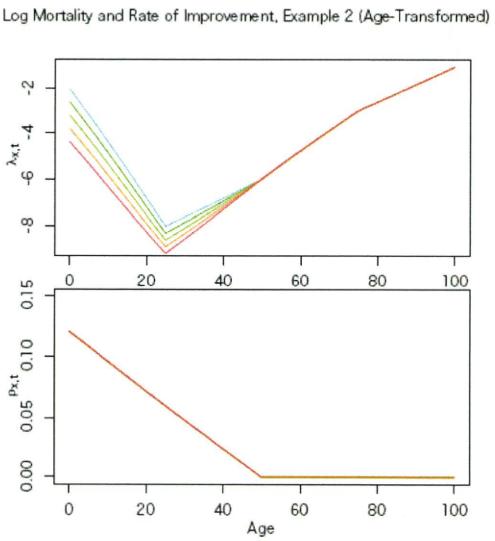

In Ishii (2008), we proposed the following age-transformation A for entire age to express the m ortality improvement as a *decline* in youn ger ag e a nd a *shift* in older a ge in o rder t o a pply the Lee -Carter procedure.

First, we fit the three parameter logistic curve

$$\mu_{x,t} = \frac{\alpha_t \exp(\beta_t x)}{1+\alpha_t \exp(\beta_t x)} + \gamma_t$$

to the actual mortality rates. Then, we obtain the parameter $S_t = -\frac{\ln(\alpha_t)}{\beta_t}$, which is used to express t he shift amount in the s hifting logistic model (Bongaarts 2005), and another parameter β_t which expresses the slope of the curve.

Next, let x be the original age and z be the transformed one, and define the relation $x = f_t(z)$ as follows.

$$f_t(z) =_{\text{def}} \begin{cases} z & (z \le B_1) \\ \left\{ \dfrac{\beta_{t_0}}{\beta_t}(B_2 - S_{t_0}) + S_t - B_1 \right\} \dfrac{z - B_1}{B_2 - B_1} + B_1 & (B_1 \le z \le B_2) \\ \dfrac{\beta_{t_0}}{\beta_t}(z - S_{t_0}) + S_t & (B_2 \le z) \end{cases}$$

Then set $\hat{\mu}_{z,t} =_{\text{def}} \mu_{f_t(z),t}$

Figure 8. Age-transformation Function
Age-Transformation

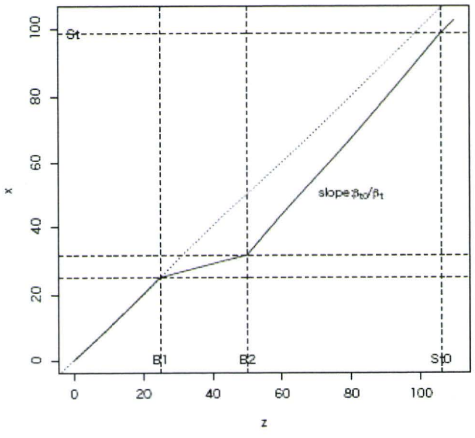

Figure 9. Iso Transformed-age Map
Iso transformed-age Map

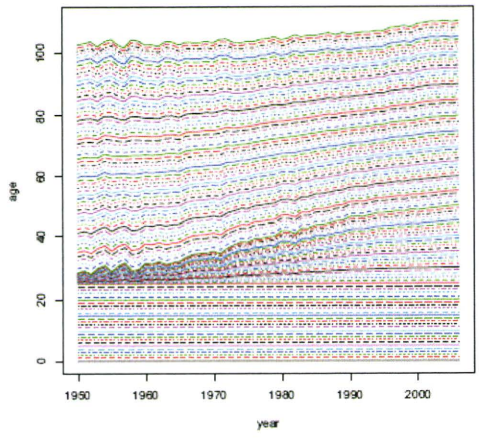

Figure 8 shows an example of age-transformation function, and Figure 9 shows the iso transformed-age map. Using the age-transformation A, modeling and projecting mortality rates are performed as $A^{-1}L\,A(\mu_{x,t})$.

4. Mortality Improvement: Decline or Shift?

In Section 3, we reviewed the age-transformation approach developed in Ishii (2008). For the modelling of adult mortality, the projection is based on the assumption that the mortality improvement is considered as shifting. It is suggested from the trends in $\mu_{x,t}$ and $l_{x,t}$ that the recent improvement in adult mortality in Japan could be better understood when considering it as shifting. In this section, we reconsider whether it is more plausible to understand mortality improvement in Japan as declining or shifting. First, we describe the definitions of the proportional hazard model and the Lee-Carter model, which are decline-type models. Then, we introduce the horizontal shifting model and the horizontal Lee-Carter model, which are shift-type models corresponding to the two decline-type ones. Through this consideration, we propose a new type of adult mortality model and discuss another way to define age-transformation.

4.1 Decline-Type Mortality Models

4.1.1 The Proportional Hazard Model (PH)

The proportional hazard model (abbreviated as PH) is a simple model that expresses mortality improvement as *decline*. In the PH model, $\lambda_{x,t}$: the log hazard rate function at time t is expressed by

$$\lambda_{x,t} = \log \mu_{x,t} = a_x + k_t$$

where ax: the baseline logged hazard rates.

In the PH model, $\rho_{x,t}$: the rate of mortality improvement

$$\rho_{x,t} = -\frac{dk_t}{dt} = -k_t^{'}$$

is constant with respect to age. This is the differential form for this model. In this paper, we fit and numerically evaluate the models against the Japanese female mortality. We use

$$m_{x,t_c}, \qquad x = x_s(=25),\ldots, x_e(=110) \text{ and } \qquad t_c = t_s(=1970),\ldots, t_e(=2007)$$

from the HMD (Human Mortality Database), where t_c is a calendar year. Here, we set a_x as the average log hazard rate in the entire period. Figure 10 shows the actual log hazard rates (λ_{x,t_c}) and the estimated rates with the PH model. We can observe that the estimated rates do not exhibit good fit particularly in the older age groups. Figure 11 shows the difference between the actual and estimated rates. From this graph, we can see that the actual values are higher than those of the model for age around from 60 to 80 in 1970, whereas these values are decreasing over time. However, opposite movement is observed for ages over 90. This is caused by the limitation of the PH model whereby the rate of mortality improvement is constant with respect to age.

Figure 10. Mortality rates (Actual and model, PH)

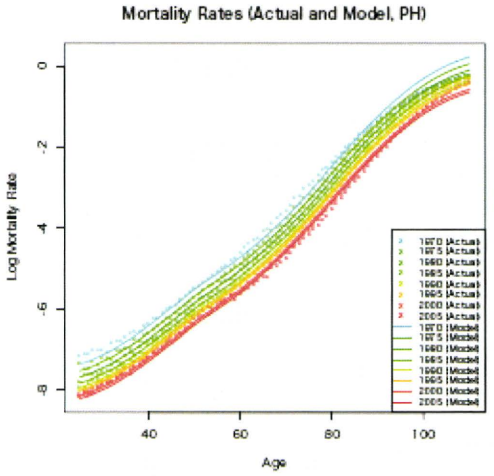

Figure 11. Difference of mortality rates (actual-Model, PH)

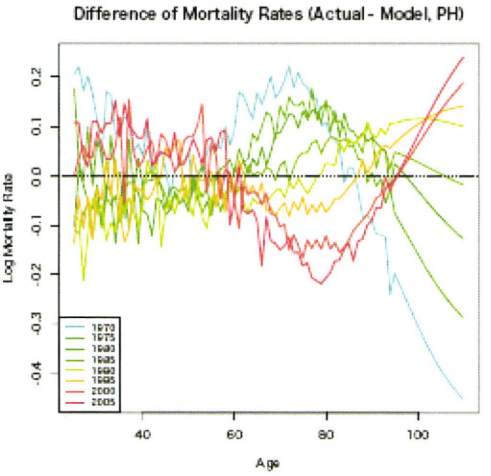

4.1.2 The Lee-Carter Model (LC)

The LC model is already defined in Section 3. It expresses mortality improvement as *decline* in a more general manner as compared with the PH model. Here, we set a_x as the average log hazard rate for the entire period. Figure 12 shows the actual log hazard rates (λ_{x,t_c}) and the estimated rates by the LC model. This figure illustrates that the fit with the actual values is fairly improved by using the LC model, due to its flexibility which admits different mortality improvement rates by age.

However, we can observe from Figure 13 that the difference between the actual and estimated rates exhibits a trend whereby the actual values are higher in younger age groups and lower in older age groups near the beginning and the end of the entire period, whereas the opposite is true around the middle of the period. The reason why this trend for the error components is observed is ascribed to the change in the age-specific mortality improvement rates over time. Therefore, we will next examine the $\rho_{x,t}$ functions for these two models.

Figure 12. Mortality rates (actual and model, LC)

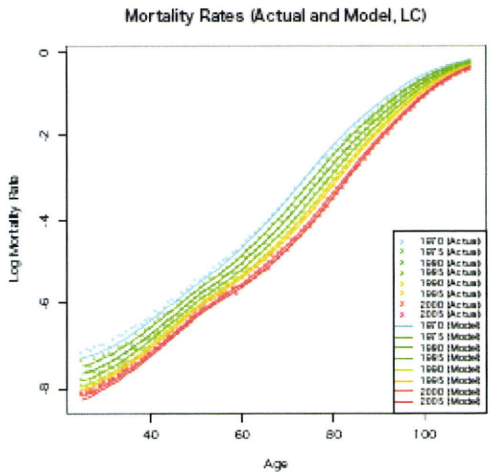

Figure 13. Difference of mortality rates (actual-model, lC)

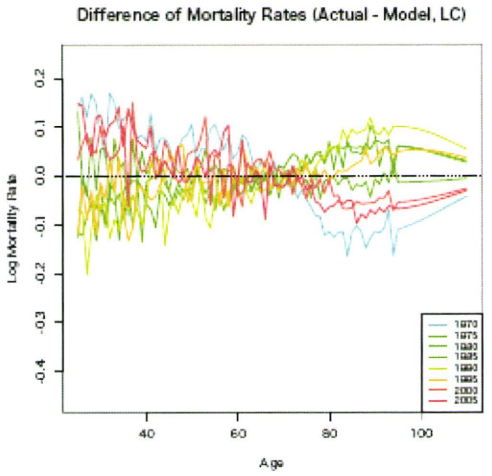

Figures 14 and 15 show the ρ_{x,t_c} functions for the actual values and the estimated values for each of the two models. The blue lines show the ρ_{x,t_c} by the actual mortality rates. We can observe that most of the mortality improvement rates have mountain-shaped curves with peaks. In contrast, the mortality improvement rates under the PH model, expressed by the pink line, are horizontal. This difference in shape would be viewed as a cause that the estimates by the PH model are not well-fitted, as we observed before. The mortality improvement rate by the LC model, indicated with the green curves, has a peak like that of the actual value, and this improves the fit as we have seen before. However, the age distribution of the rates is fixed in the LC model, whereas it changes dynamically in the actual values. Thus, the actual age distribution of mortality improvement rates change over time and are not constant as in the LC model, and caused the propensity for the error in the LC model observed in Figure 13. We could see this result as a limitation when the mortality improvement is considered as *decline*.

Figure 14. Comparison of mortality improvement rates (1974-1989)

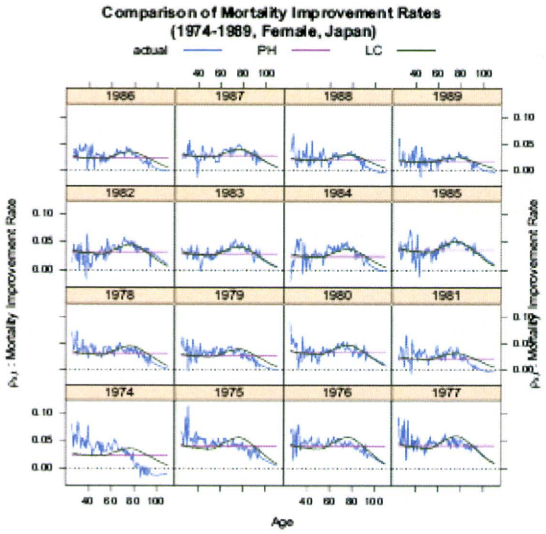

Figure 15. Comparison of mortality improvement rates (1990-2005)

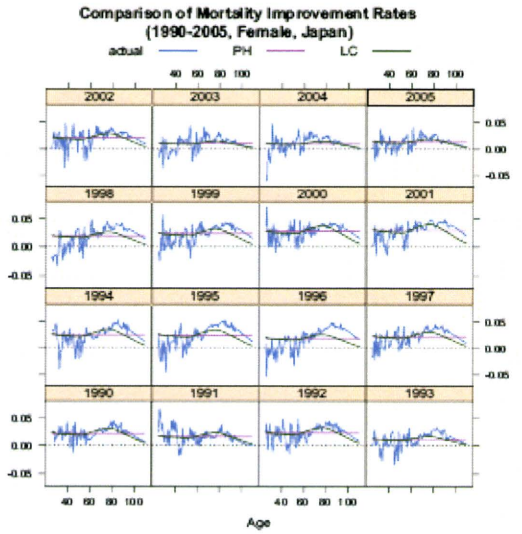

4.2 Shift-Type Mortality Models

4.2.1 The Horizontal Shifting Model (HS)

Next, we discuss models that express mortality improvement through a *shift*. The simplest model for *shifting* would be one whereby the entire log hazard curve moves to the right-hand side. We can restate this model using the inverse function of log hazard mortality $v_{y,t}$, that is, the proportional hazard model for $v_{y,t}$.

This model that we call the horizontal shifting model (abbreviated as HS) here is formally expressed as follows:

$$v_{y,t} = a_y + k_t$$

In the differential form,

$$\tau_{y,t} = \frac{dk_t}{dt} = k_t^{'}$$

Parameter estimation for the HS model is completely identical to the PH models, except for adapting these procedures to v_{y,t_c} instead of λ_{y,t_c}. Figures 16 and 17 are the actual inverse mortality rates (v_{y,t_c}) and the estimated rates by the HS model, and the difference between the actual and the estimated. We can see that the performance of fitting by the HS model is much better than by the PH model, even though both have the same structure. For 1970, indicated with the light blue line, the actual values are higher in younger ages and lower in older ages, though the errors are not as high for other years.

Figure 16. Inverse mortality rates (actual and model, HS)

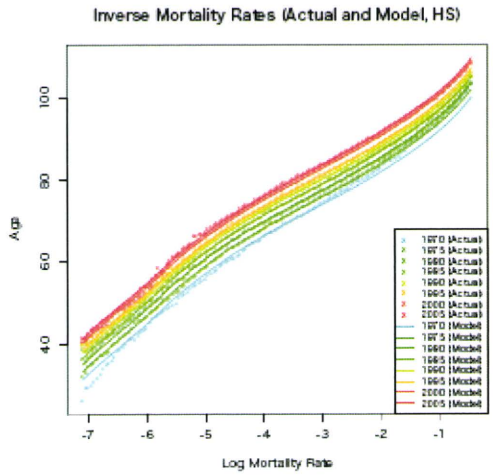

Figure 17. Difference of inverse mortality rates (actual and model, HS)

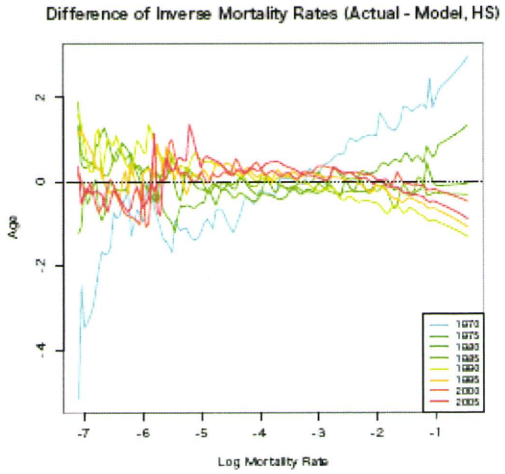

4.2.2 The Horizontal Lee-Carter Model (HL)

As we considered the LC model which admits a different amount of decline by age and provides a more general framework compared with the PH model, we can also consider the Lee-Carter model for $v_{y,t}$ which in turn supports a more general shifting feature. We call it the horizontal Lee-Carter model (abbreviated as HL).

$$v_{y,t} = a_y + k_t b_y$$

In the differential form,

$$\tau_{y,t} = \frac{dk_t}{dt} b_y = -k_t' b_y$$

Figures 16 and 17 are the actual inverse mortality rates (v_{y,t_c}) and the estimated rates under the HS model, and the difference between the actual and the estimated. We can see that the HL model seems to be improved compared to the HS model. However, it is also observed that the improvement between the *shift* pair is not as large as the *decline* pair. This means that relaxing the limitation, which the force of age increase in the HS model is restricted to the constant function, does not cause significant improvement of fit in the HL model. It could be explained by the difference in the shape of τ_{y,t_c}, the force of age increase. Figures 20 and 21 show the τ_{y,t_c} functions for the actual values and the estimated values by the two shifting models. We observe that the green curves, which correspond to τ_{y,t_c} by the HL model, are close to a horizontal line, which coincides with the force of age increase by the HS model shown in the pink lines. This fact endorses that the improvement between the *shift* pair is not as large as the decline pair.

Figure 18. Inverse Mortality Rates (actual and model, HL)

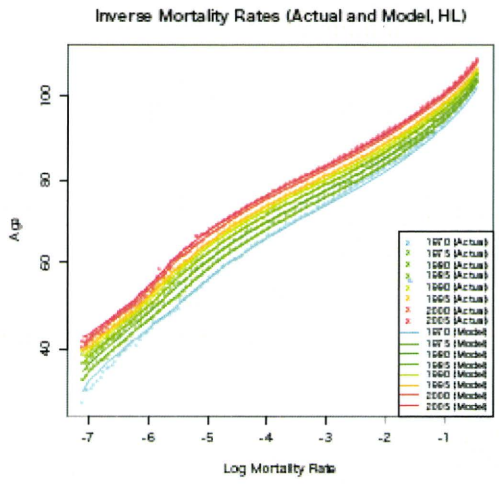

Figure 19. Difference of Inverse Mortality Rates (actual and model, HL)

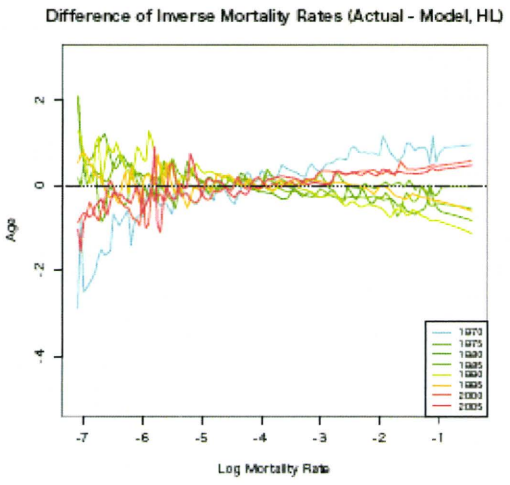

However, from the observation of these figures, we have noticed that the blue lines for the actual τ_{y,t_c} for each year could be more well-modelled by a linear function of y, which has led us to the development of a new model: the linear difference model. We will define and examine this new model in the next section.

Figure 20. Comparison of the force of age increase by log mortality rate (1974-1989)

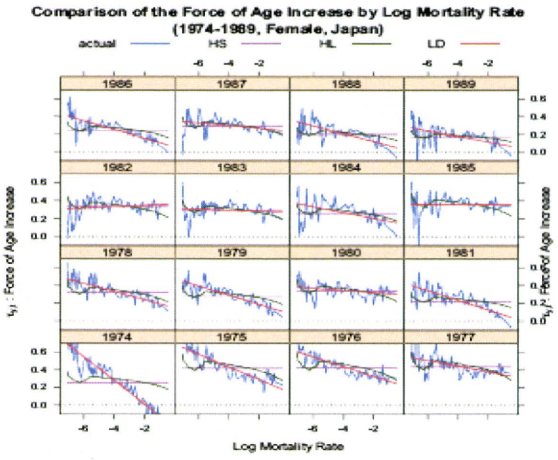

Figure 21. Comparison of the force of age increase by log mortality rate (1990-2005)

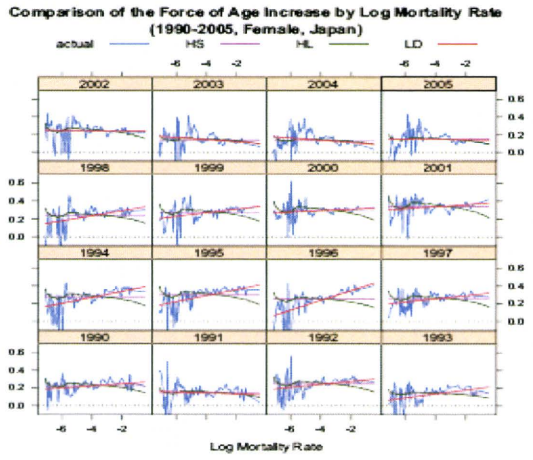

4.3 The Linear Difference Model (LD)

First, we describe the linear difference model (abbreviated as LD) in the continuous form as we did in other models. In the LD model, we assume that $\tau_{y,t}$ is a linear function of y for each t.

$$\tau_{y,t} = k_t^{'} + c_t^{'} y$$

This is the differential form. By integrating both sides with t, we obtain

$$v_{y,t} = k_t + c_t y + a_y$$

where a_y denotes a standard pattern of inverse log hazard rates.

Figures 22 and 23 are the actual inverse mortality rates and the estimated rates by the LD model, and the difference between the actual and the estimated. From these figures, we can observe that the LD model fits quite well with the actual values.

This is also confirmed from the observation of $\tau_{y,t}$ functions in Figures 20 and 21. We can observe that the linear assumption for τ_{y,t_c} in the LD model works better than in the other two models.

Figure 22. Inverse mortality rates (actual and model, LD)

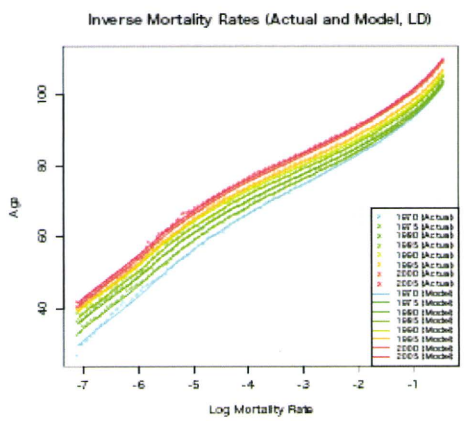

Figure 23. Difference of inverse mortality rate (actual and model, LD)

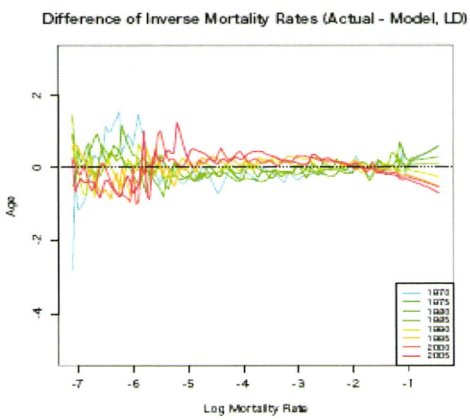

4.4 Comparison of the Models from a Statistical Viewpoint

In this section, we compare the LC and LD models from a statistical viewpoint to examine whether it is more plausible to understand the recent Japanese mortality as *declining* or *shifting*. Our approach is as follows.

1. The true mortality rates are assumed to be those that are estimated by models.

2. The number of deaths follows a binomial distribution $B(N_{x,t_c}, p_{x,t_c})$, where N_{x,t_c} : the number of the population and p_{x,t_c} : the death rate for age x and calendar year t_c.

3. N_{x,t_c} is approximated by the closest integer to E_{x,t_c} : exposure to risk.

Here, we took 0 .01% as a cr itical v alue to co nstruct th e confidence in tervals (CI), sin ce $N_{x,t}$ would present too large value for the Japanese female population. Figure 24 shows the proportion where the log actual mortality rates are outside of the CIs for eac h age in the LC and LD models. This indicates tha t even though the proportions of LD are higher for certain ages, LD's performance would be considered as fairly better than LC's as a whole. This result suggests that *shift* is more strongly supported as recognition of the recent mortality improvement in Japan than *decline*.

Figure 24. proportion that log actual values are outside of CI (critical value=0.01%)

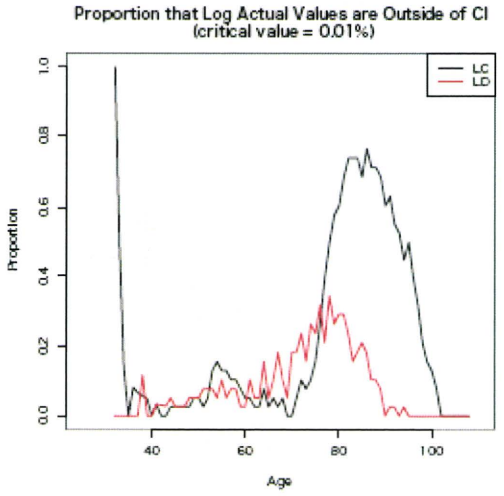

Figure 25. log mortality surface and two differential functions.

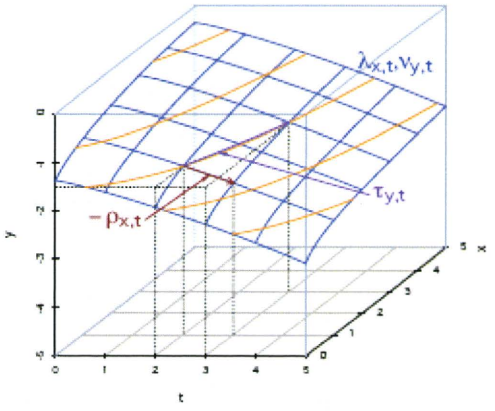

4.5 Differential Forms and Age-transformations

Next, we consider the relationship between differential forms and a ge-transformations, and discuss how the LD model is related to the age-transformation approach.

In section 1, we defined $\rho_{x,t}$ and $\tau_{y,t}$ on the log mortality surface *S*. Then, the vectors

$$\rho(x_0,t_0,y_0)=(0,1,-\rho_{x_0,t_0})$$

$$\tau(x_0,t_0,y_0)=(\tau_{y_0,t_0},1,0)$$

are tangent vectors on *S* as shown in Figure 25. Each tangent vector defines a tangent vector field on *S*. In general, an is o-transformed age m ap is defined by the proj ection of the integral curve induced by the tangent vect or field onto a *X-T* plane. For exam ple, the iso-transformed a ge m ap ind uced by ρ is an identity age-transformation, and one by τ is an age-transformation that id entifies the ages that yield the same log hazard rates. If we define another tangent vector field on *S*, then another iso-transformed age map is induced. Therefore, a tangent vector field on *S* is considered as another representation of an age-transformation.

Let us recall that the LD model is defined by a differential form that is a modeling of $\tau_{y,t}$. Therefore, the LD model defines an age-transformation through the vector field interpretation with a tangent vector τ. This relationship relates the LD model to the age-transformation approach.

5. Concluding Remarks

In this paper, we examined and proposed a new method for mortality projection for Japan as an application of the age-transformation approach.

We considered which is more plausible to understand mortality improvement in Japan as decline or shift. First, we described the definitions of the proportional hazard model and the Lee-Carter model, which are *decline*-type models. Then, we introduced the horizontal shifting model and the horizontal Lee-Carter model, which are *shift*-type models corresponding to the two *decline* type ones. Next, we noticed that the actual τ_{y,t_c} for each year could be well-modelled by a linear function of y, and proposed the linear difference (LD) model. We observed that the LD model coincided quite well with the actual values.

Then, we compared the LC and LD models from a statistical viewpoint to examine whether it is more plausible to understand the recent Japanese mortality as a *decline* or *shift*. We observed that LD's performance would be considered advantageous over LC's as a whole. This result suggests that *shift* is more strongly supported as recognition of the recent mortality improvement in Japan than *decline*.

Finally, we considered the relationship between differential forms and age-transformations, and discussed how the LD model is related to the age-transformation approach. In general, an iso-transformed age map is defined by the projection of the integral curve induced by the tangent vector field onto $X - T$ plane. Therefore, a tangent vector field on S is considered as another representation of an age-transformation. The LD model is defined by a differential form that is a modelling of $\tau_{y,t}$. Therefore, the LD model defines an age-transformation through vector fields interpretation with tangent vector $\boldsymbol{\tau}$. This relationship relates the LD model to the age-transformation approach.

In this paper, we confirmed that the LD model is efficient, although we noted further points that should be examined. First, we discussed only the adult mortality model here, whereas the entire age model should be developed. Second, we focused on the modelling of the actual values in this paper, whereas we should consider how to project the parameters. These points should be studied in future.

References

Bongaarts, J. (2005) "Long-range Trends in Adult Mortality: Models and Projection Methods", *Demography*, Vol. 42, No. 1, pp. 23–49.

Human Mortality Database. University of California, Berkeley (USA) and Max Planck Institute for Demographic Research (Germany). Available at www.mortality.org or www.humanmortality.de.

Ishii, F. (2008) "Mortality Projection Model for Japan with Age-Shifting Structure", Paper presented at 2008 Annual Meeting of Population Association of America (New Orleans).

Lee, R. and L. Carter (1992) "Modeling and Forecasting U.S. Mortality", Journal of the American Statistical Association, Vol. 87, No. 419, pp. 659–675.

NIPSSR (2007) Population Projections for Japan: 2006-2055 (With long-range Population Projections: 2056-2105).